Colloid and Polymer Science (2021) 299:153–164
https://doi.org/10.1007/s00396-020-04775-5

ORIGINAL CONTRIBUTION

Fatty acid-peptide-bioconjugated micellar nanocarrier as a new delivery system for L-asparaginase: multi-criteria optimization, characterization, and pharmacokinetic study

Hajar Ashrafi[1] · Amir Azadi[1,2] · Soliman Mohammadi-Samani[1,2] · Younes Ghasemi[2,3] · Saeid Daneshamouz[1]

Received: 11 August 2020 / Revised: 15 October 2020 / Accepted: 21 October 2020 / Published online: 5 November 2020

Abstract

L-Asparaginase-fatty acid bioconjugate was prepared by coupling the carboxyl group of fatty acids to NH_2 groups of lysine of the enzyme. In this study, the physicochemical properties of L-asparaginase were modified by incorporating surfactant with this amphiphilic structure. The preparation process of micellar nanocarrier was optimized by a systematic multi-criteria optimization approach in terms of particle size and enzyme activity. The final particle size, PDI, and enzyme activity were 387.6 ± 9.8 nm, 0.341 ± 0.031, and 92.1 ± 1.3%, respectively. Results are in an optimum condition. Furthermore, results showed that the optimized formulation is more resistant to proteolysis, is more stable at different pH (6.5 to 10), and has prolonged plasma half-life (56.8 h) in comparison to the native enzyme. Also, the longevity in the circulation by micellar nanocarriers was confirmed by the data on the pharmacokinetic study. This method can be used as a suitable method to provide a new formulation of L-asparaginase for the treatment of related diseases.

Keywords L-Asparaginase · Lipid-protein conjugation · Multi-criteria optimization · Pharmacokinetic

Introduction

L-Asparaginase (L-ASNase) is one of the most efficient drugs in the treatment of lymphoblastic leukemia [1–3]. Today, *Escherichia coli* strains or *Erwinia chrysanthemi* are the two primary sources of L-ASNase [4, 5]. Until recently, attempts were made to increase in vitro and in vivo efficacy of L-ASNase, for instance, its biological half-life, stability, and reduced antigenicity. One successful approach is the chemical modification of L-ASNase, which leads to an increase in enzyme stability by prolonging its biological half-life [6, 7]. Colominic acid is one such compound when conjugated with L-ASNase reduces antigenicity, leading to circulatory half-life 3–4-fold higher than the native enzyme [8]. Silk fibroin, silk sericine [9, 10], oxidized inulin [11], *N*,*O*-carboxymethyl chitosan [12], and carboxymethyl dextran [13] are the other biocompatible compounds. In addition to that, some other nanoparticulate systems are also used for conjugation [14, 15] or immobilization of L-ASNase [16, 17]. Recently, our research group presented a L-ASNase-fatty acid bioconjugate with three types of fatty acids with different chain lengths (i.e., lauric acid, palmitic acid, and behenic acid) [18]. Our results revealed excellent stability for the conjugated enzyme by/and improvement in its in vitro half-life and enzyme affinity to its substrate.

We proposed a binary micellar system, in which surfactants were added to L-ASNase-fatty acid bioconjugate. This structure has presented physicochemical properties different from the native form, which was investigated in this experiment [19]. Over the last decades, the development of mixed micelle among the variety of surfactants [20], fatty acids/surfactants [21], and other amphiphilic polymers has been observed. In this experiment, we attempted to explore the optimum conditions for obtaining micellar nanocarriers with small particle size, while maintaining high residual activity, using statistical response surface methodology. The optimization method was

✉ Saeid Daneshamouz
daneshamuz@sums.ac.ir

[1] Department of Pharmaceutics, School of Pharmacy, Shiraz University of Medical Sciences, Shiraz, Iran

[2] Pharmaceutical Sciences Research Center, Shiraz University of Medical Sciences, Shiraz, Iran

[3] Department of Pharmaceutical Biotechnology, School of Pharmacy, Shiraz University of Medical Sciences, Shiraz, Iran

performed in its traditional way by changing one parameter at the same time while others were kept constant at a fix level, but it is time consuming. In contrast, with experimental design, a researcher can efficiently determine the effects of a factor with significantly less experimental effort and identify factors, find optimum condition, offer greater precision [22], and facilitate system modeling [23, 24]. Consequently, a series of in vitro characterization test were carried out on the optimized micellar nanocarriers to evaluate their potential impact on the final step of in vivo investigations in animal models.

Materials and methods

Materials

L-Asparaginase from *E. coli* strain with a molecular weight of 140 kDa was obtained from Medac®, Hamburg, Germany. The palmitic and lauric acid used for conjugation were from Merck Co. (Darmstadt, Germany), and behenic acid was purchased from Fluka Co. Ltd. (Buchs, Switzerland). Other analytical-grade chemical reagents were purchased from Sigma (St. Louis, MO, USA) or purchased locally.

Synthesis of L-ASNase-fatty acid bioconjugate

The carboxylic group of three types of fatty acids with different chain lengths (i.e., lauric acid, palmitic acid, and behenic acid with 12, 16, and 22 chain lengths) were conjugated with the amine group of lysine in L-ASNase using carbodiimide activator [25]. At the first step, 3.57 μmol of fatty acids dissolved in 5 mL of dimethyl sulfoxide (DMSO). Then, 3.93 μmol *N*-(3-dimethyl aminopropyl)-*N*-ethyl carbodiimide-hydrochloride (EDC) and 3.57 μmol *N*-hydroxysuccinimide (NHS) were added to the mixture. The mixture was stirred at 25 °C for 3 h. Then, 0.0714 μmol of L-ASNase in 5 mL of water was added to the mixture dropwise. After the reaction time, unreacted lipid, EDC, NHS, and DMSO were removed by dialysis (12 kDa) against an excessive amount of water for 24 h. Differential scanning calorimetry and calorimetric method are used to determine the efficacy of dialysis for removing unreacted fatty acids [26]. After this, samples were lyophilized for 48 h using a freeze drier (Christ, α1-4 LD plus, Germany). All experiments were performed in triplicate.

Micellar preparation of the bioconjugate

Preliminary study for surfactant selection

To obtain nanomicellar structures of the L-ASNase-fatty acid bioconjugate, several groups of surfactants were utilized and their effects on enzyme activity retention and particle size of resulted micellar nanocarriers were evaluated. The surfactants were in different HLB values and alkyl chain of nonionic (Brijs: 35, 52, 92, 72; Tweens: 20, 40, 60, 80; Spans: 20, 40, 60, 85, 83; Pluronics: F-127, F-68, and Triton X-100), anionics (sodium lauryl sulfate and sodium cholate), cationic (cetyl pyridinium chloride), and soybean lecithin.

At a preliminary step, an appropriate amount of the surfactants was dispersed in distilled water and added to about 10 mL of bioconjugate suspension (1 mg/mL of enzyme), to prepare a concentration above the critical micelle concentration (CMC) value of that surfactant, while stirring at room temperature for 60 min [27]. For lyophilization, the total volume of the resulting micelles was divided into different containers with a liquid depth of about 1 cm and was lyophilized for 48 h.

Experimental design

Throughout the present study, a systematic multi-criteria optimization approach used for the optimization of the micellar nanocarrier preparation in terms of the final particle size and enzyme activity of the resulting micelles after the reconstitution of lyophilizate.

Optimization

A D-optimal design planned to determine the best experimental conditions for the preparation of micellar nanocarrier. This design uses the points that minimize the variance associated with the estimates of the specified model coefficients. This design scientifically settles to declare the most accurate estimates of the model equations. The D-optimal design was used for the best model fitting of the test data. The data was analyzed by using the Design-Expert statistical software (version 6.0.10, Stat-Ease Inc., Minneapolis, USA), which was used for the generation of the experimental design matrix. In this design, a statistical model suggested on describing the effects of preparation conditions based on the data of micellar nanocarrier particle size and enzyme activity. Next, a stepwise regression model was employed to fit the polynomial model to the data [28]. For detection of outliers, the normal probability plot and Cook's distance were tested. A lack-of-fit test with the analysis of variance (ANOVA) model, a plot of the predicted values versus residuals, leverage, and a graphical diagram of the predicted versus experimental data proved the suitability of the models. The interaction plots were prepared to analyze the optimum conditions for the dependent variables. The factors and the corresponding levels involved in the study are shown in Table 1.

Table 1 Applied levels of independent variables in D-optimal design

Factor	Name	Type	Low actual	High actual	Low coded	High coded
A	Lipid/protein	Numeric	50	200	− 1	+ 1
B	Lipid type	Categorical	Lauric acid; palmitic acid; behenic acid		B [1]	B [2]
					+ 1	0
					0	+ 1
					− 1	− 1
C	Surfactant type	Categorical	Pluronic F-127; sodium cholate		− 1	
					+ 1	

Preparation of optimum micellar nanocarrier

In the optimum condition, an appropriate amount of pluronic F-127 was dispersed to the bioconjugate suspension to prepare a 0.79-mM (i.e., 1%, *w*/*v*) concentration while stirring at room temperature for 60 min for equilibration. In this condition, the concentration of L-ASNase was 1 mg/mL (i.e., 0.1%, *w*/*v*). The resulting micellar nanocarriers were frozen at − 70 °C and then freeze dried. The freeze-dried samples were then subjected to further evaluations.

Determination of suitable surfactant concentration

To evaluate the effect of surfactant concentration (Pluronic F-127) on the bioconjugated enzyme activity and particle size of the micelles, three different concentrations (below the CMC value, CMC value, and above the CMC value) of the surfactant were tested.

Assay methods

Two colorimetric methods were used to evaluate the degree of modification in lysine residues in the native and bioconjugate enzymes [29, 30]. Ninhydrin and TNBS can bind to the free amine group of lysine from the native and modified enzyme, so the degree of chemical modification of the enzyme could be evaluated [10]. In this study, Nessler's reagent was used to quantify the ammonia for in vitro experiments [31, 32], which are the byproduct of L-asparagine activity. Bradford protein assay was used to determine the protein concentration in vitro [33] in the concentration range of 0.25–20 μg/mL.

In vitro characterization tests

Stability against proteolysis and determination of pH-activity profile

The given amounts of the micellar nanocarriers were added to 2 mL phosphate-buffered solution (pH 8.5) containing 50 IU trypsin. Then, the residual enzyme activity of each sample was measured at time points of 10, 20, 30, 40, and 60 min after incubation at 37 °C. All data were the average values of triplicate measurements.

The influence of pH on the activity of micellar nanocarriers were studied by changing the pH from 3 to 12. The incubation of the enzyme determined the enzyme activities in phosphate buffer (0.05 M) in different ranges of pH. All experiments were performed in triplicate.

Kinetic measurements and time-activity profile in PBS and plasma

In the kinetic study, the Michaelis constant (K_m) from the Lineweaver–Burk equation [34] was used as a parameter to determine the affinity of the native and micellar nanocarrier for the substrate. Different L-asparagine concentrations (0.4 to 2 mM) in 0.05 M tris buffer, pH 8.5 was used to measure the K_m value. All experiments were performed in triplicate.

Catalytic activity and enzyme in vitro half-life of the micellar nanocarriers were determined by using phosphate-buffered saline (PBS, pH 7.4) and human plasma. For this test, equivalent preparations (1 mg of the optimized formulation) were added into 2 mL of PBS or plasma. Then, samples were incubated at 37 °C for 0, 1, 2, 4, 8, 10, 12, 24, 48, 72, 96, 168, and 336 h. After that, 0.1 mL of each sample was taken at mentioned time intervals and analyzed for their in vitro catalytic activity. All experiments were performed in triplicate.

Determination of CMC, particle size, size distribution, and surface charge

The surface tension of surfactant and micellar nanocarriers was measured by the DuNouy ring tensiometer (KSV's Sigma 702 instrument). The platinum ring used in the measurements was cleaned by washing with ultrapure water (Millipore) followed by washing with *n*-hexane and acetone. The surface tension of double-distilled water used for calibration purposes was 71.85 mN/m at 25.0 ± 0.1 °C. The CMC values were then obtained through a conventional plot. In this method, the surface tension was plotted versus the logarithm value of the surfactant concentration.

The mean diameter of the nanocarriers was measured by a laser diffraction approach using a particle size analyzer (Shimadzu, model SALD-2101, Japan). Samples were reconstituted to appropriate concentrations (0.1 mg/mL) with distilled/filtered water. Measurements were conducted at 25 °C. Zeta potential measurements were also performed using the Malvern Zetasizer (Zetasizer V-R 3000-HS, Malvern Instruments, UK) which operates based on electrophoretic light scattering technique.

Morphology

The morphology and possible aggregation of the optimized formulation (behenic acid bioconjugate/pluronic F-127) were characterized using transmission electron microscopy (TEM) (Zeiss, model EM10C, Germany). For imaging, samples were fixed on the copper grids, dried at room temperature, and examined using a TEM without being stained.

Pharmacokinetic analysis

Twenty-one adult male Sprague-Dawley rats (about 200–250 body weight) were divided into three groups ($n = 7$); A cocktail of ketamine-xylazine (ketamine 100 mg/kg and xylazine 10 mg/kg) was used to anesthetize the rats through IP injection. Rats were then cannulated by inserting a polyethylene-silicone rubber cannula into the right jugular vein using a standard surgical protocol [35]. Rats were then placed in clean single cages and left overnight for complete recovery. The animals were cared for according to the instructions of the ethics committee of Shiraz University of Medical Sciences. Native L-ASNase, behenic acid bioconjugate, and optimum micellar nanocarrier formulation (behenic acid bioconjugate/pluronic F-127) with a dose of 10 mg/kg (2500 IU/kg) prepared in sterile saline. The animals in each group were given one dose of each formulation intravenously. Blood samples were aseptically collected after intervals of 0, 1, 2, 4, 6, 8, 12, 24, and 48 h, and serum were isolated. Normal rat serum (NRS) obtained from rats, which had never received L-ASNase was used as a negative control.

For in vivo quantification of the enzyme activity, the commercially available L-ASNase activity assay kit (Abnova Company, Cat #KA1429) was used. The L-ASNase concentration from the pharmacokinetic study was determined using the manufacturer's specified protocol.

Statistical analysis

The significance of the observed differences between the data sets was evaluated statistically using the statistical t test and one-way ANOVA, the statistical non-parametric Mann-Whitney U test, and Kruskal-Wallis one-way analysis of variance (SPSS 16.0; SigmaPlot 11.0) whenever applicable at a significance level of 0.05.

Results and discussion

Synthesis of L-ASNase-fatty acid bioconjugate

In this study, three different chain lengths of fatty acid conjugated with L-ASNase were synthesized. The carboxylic group of the fatty acids was conjugated with the amine groups of lysine and N-terminal amino groups of the enzyme. The improved properties of L-ASNase-fatty acid bioconjugate were characterized as reported previously by the authors [18].

Preparation of micellar nanocarriers

Preliminary study for surfactant selection

In this study, among different surfactants mentioned before ("Preliminary study for surfactant selection"), pluronic F-127, and sodium cholate provided the smaller particle size and higher enzyme activity than other agents throughout the procedure. To find the suitable surfactant (between pluronic F-127 and sodium cholate) for the preparation of fatty acid bioconjugated micellar nanocarrier, a D-optimal design was utilized through the 19 experiments.

Experimental design

The classical method of optimization based on changing one parameter at a time while keeping the others at fixed levels is laborious and time consuming. This method requires a complete series of experiments for each factor of interest. Moreover, such a method does not provide a complete overview of possible interactions between the different factors. Contrary to the classical method, factorial experimental design is advantageous. For instance, the researcher could simply control the effects of a factor that has considerably less experimental effort, identify factors, find optimum condition, offer greater precision [22], and facilitate system modeling [36]. Table 2 shows the design and results of the experiments carried out throughout the D-optimal design.

Particle size optimization

The particle size obtained from all 19 experiments was fitted to polynomial models according to Cook's distances with no detectable outliers. No data transformation was done. The F value of the model ($F = 8.04$) shows that the model is significant. Also, it is not significant based on the lack-of-fit test, relative to the pure error (P value = 0.1386). The relatively high R-squared (0.9096) and adjusted R-squared (0.7965)

Table 2 Experimental design matrix and results of D-optimal design

Run No.	Lipid/pr	Lipid type	Surfactant type	Particle size (nm)	Enzyme activity %
1	162.5	Behenic acid	Pluronic F-127	615 ± 106	92.3 ± 6.3
2	50	Behenic acid	Sodium cholate	471 ± 61	71.6 ± 4.8
3	50	Lauric acid	Sodium cholate	417 ± 2	69.3 ± 2.9
4	162.5	Palmitic acid	Sodium cholate	643 ± 100	44.8 ± 3.2
5	200	Palmitic acid	Pluronic F-127	732 ± 46	78.4 ± 0.5
6	200	Behenic acid	Sodium cholate	636 ± 43	62.0 ± 0.8
7	87.5	Lauric acid	Pluronic F-127	491 ± 104	82.7 ± 8.0
8	87.5	Palmitic acid	Pluronic F-127	482 ± 60	85.6 ± 8.2
9	200	Lauric acid	Sodium cholate	607 ± 74	43.0 ± 1.1
10	50	Behenic acid	Pluronic F-127	435 ± 14	98.0 ± 3.3
11	50	Palmitic acid	Sodium cholate	456 ± 41	56.1 ± 3.8
12	200	Lauric acid	Pluronic F-127	823 ± 91	79.0 ± 2.3
13	125	Lauric acid	Sodium cholate	687 ± 22	41.4 ± 3.3
14	125	Behenic acid	Sodium cholate	696 ± 15	63.8 ± 7.7
15	50	Lauric acid	Pluronic F-127	428 ± 28	71.9 ± 2.6
16	50	Palmitic acid	Sodium cholate	469 ± 64	50.2 ± 6.6
17	200	Palmitic acid	Pluronic F-127	720 ± 54	70.1 ± 8.3
18	200	Behenic acid	Sodium cholate	621 ± 25	63.0 ± 6.7
19	162.5	Palmitic acid	Sodium cholate	752 ± 9	35.3 ± 5.4

values indicated an acceptable correlation between the test data and those of the fitted models. The software offered the final mathematical modeling in terms of coded factors for the micellar nanocarrier particle size that developed as follows, where *A*, *B*, and *C* are "lipid/protein ratio," "lipid type," and "surfactant type," respectively:

$$\begin{aligned}\text{Particle size} = {} & 642.20 + 134.37A + 11.16B[1] - 3.97B[2] \\ & + 8.24C - 87.21A2 + 20.49AB[1] \\ & + 23.61AB[2] - 38.18AC - 33.13B[1]C \\ & + 17.99B[2]C \end{aligned} \quad (1)$$

The interaction graphs are shown in Fig. 1a–c based on the particle size of the final model. Figure 1a shows the interaction between the lipid/protein ratio and lipid-type factors. The particle size is increasing while varying the lipid/protein ratio to higher levels in its experimental range. This phenomenon is observable for all lipid types. On the other hand, mixed micelles prepared from lauric acid bioconjugate have a larger particle size in comparison to palmitic and behenic acid ones. Behenic acid bioconjugate mixed micelles do not show parallel behavior through the lipid/protein experimental range with the other two. Also, as seen in Fig. 1b, particle size is increasing with both surfactant types by increasing the lipid/protein levels. However, in lower lipid/protein ratios, pluronic F-127 has led to smaller micelles. This graph demonstrates the interaction between surfactant type and lipid/protein factors. Moreover, palmitic and behenic acid bioconjugate mixed micelles have a smaller particle size with pluronic F-127, while mixed micelles prepared by lauric acid bioconjugate have presented their smaller size by sodium cholate surfactant (Fig. 1c).

Enzyme activity optimization

The enzyme activity obtained for all 19 experiments are fitted to polynomial models with no detectable outliers according to Cook's distances. No data transformation was done. The *F* value of the model ($F = 10.13$) indicates that the model is significant. Also, the lack-of-fit test revealed that it is not significant relative to the pure error (*P* value = 0.1382). The relatively high *R*-squared (0.9268) and adjusted *R*-squared (0.8352) values implied that there is a good relationship between experimental data and appropriate models.

The final mathematical modeling in terms of coded factors offered by the software for the mixed micelles enzyme activity developed as follows, where *A*, *B*, and *C* are "lipid/protein ratio," "lipid type," and "surfactant type," respectively:

$$\begin{aligned}\text{Enzyme activity} = {} & 67.34 - 5.19A - 4.81B[1] - 6.94B[2] - 15.16C \\ & + 2.56A2 - 0.26AB[1] - 2.23AB[2] - 2.91AC \\ & + 2.16B[1]C - 2.82B[2]C \end{aligned} \quad (2)$$

According to the interaction graph obtained from the enzyme activity final model, it was obvious that in the

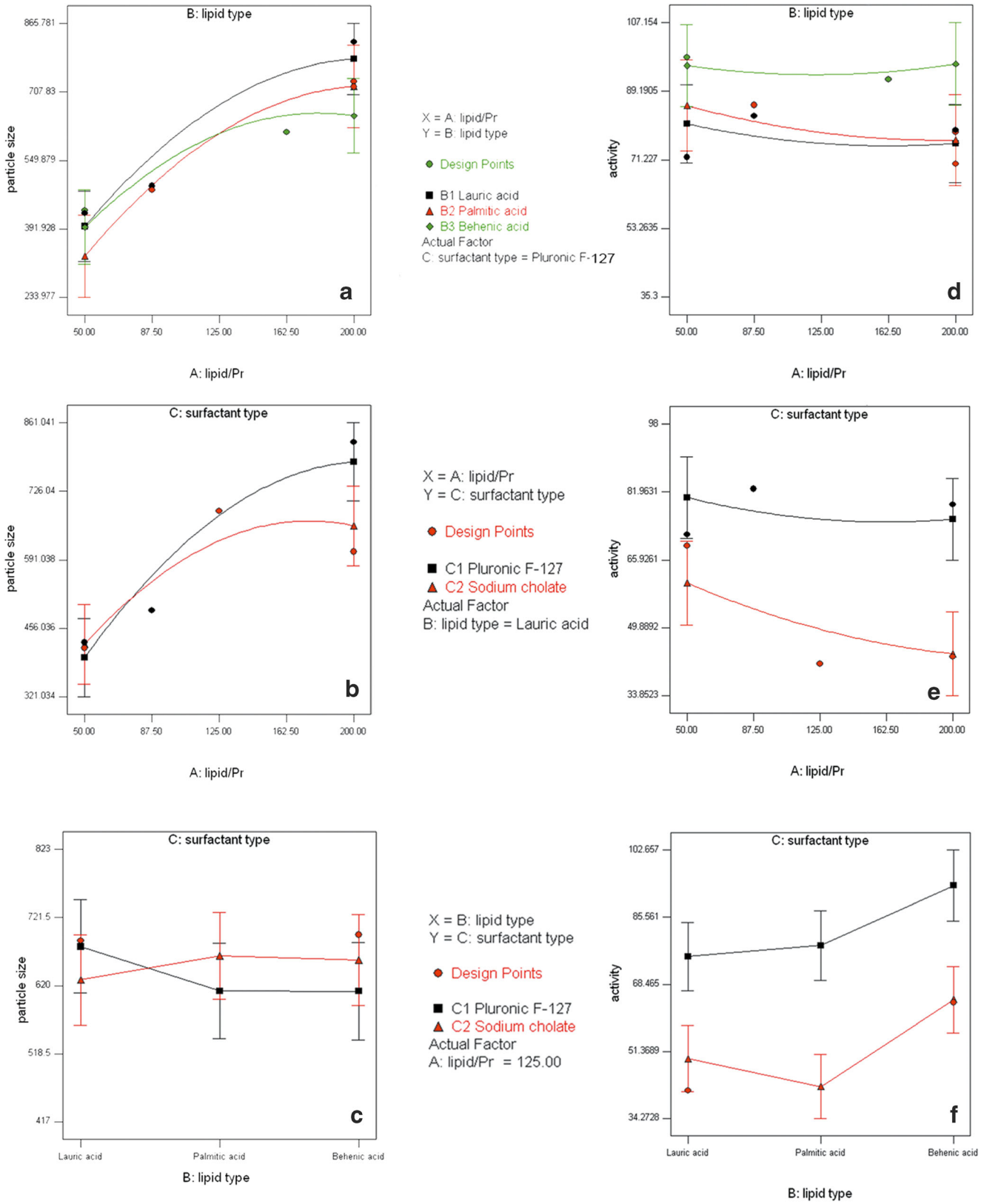

Fig. 1 Interaction plots; **a** interaction between lipid/protein ratio and lipid-type factors based on particle size; **b** interaction between surfactant-type and lipid/protein factors based on particle size; **c** interaction between surfactant-type and lipid-type factors based on particle size; **d** interaction between lipid/protein ratio and lipid-type factors based on enzyme activity; **e** interaction between surfactant-type and lipid/protein factors based on enzyme activity; **f** interaction between surfactant-type and lipid-type factors based on enzyme activity

experimental range of lipid/protein factor, the activity of longer chain lipid bioconjugate was higher than shorter ones (Fig. 1d). It can be due to the protective effect of these lipid chains on the enzyme bioactivity via steric hindrance. This phenomenon was seen in the bioconjugtion process too. Moreover, the mixed micelles prepared with pluronic F-127 also had a higher enzyme activity compared with the sodium cholate mixed micelles (Fig. 1e). The enzyme activity decrement by increasing the lipid/protein levels is notable in this graph. Figure 1f is an informative graph. It can conclude that the pluronic F-127 led to less activity reduction compared with the sodium cholate. On the other hand, almost in all cases, the activity was increased with longer chain lipids, as described earlier. From these interaction graphs, one can conclude that the pluronic F-127 and behenic acid bioconjugate have relatively more acceptable results.

Multi-criteria optimization

The main goal in the optimization studies is the identification of the experimental conditions, which results in the best responses. However, dependent variables may sometimes be antithetical, and accommodation of optimal condition between them is needed. To overcome this problem, in a process known as a multi-criteria optimization (MCO), desirability functions are used [37]. This approach was first introduced by Derringer and co-workers [38]. The Derringer's desirability or "*D*" was characterized as the geometric mean of the individual desirability values. The Derringer's desirability function id defined as follows:

$$D = [d1 \times d2 \times \ldots \times dn]1/n \; 0 < \mathrm{D} < 1 \qquad (3)$$

where n is the number of responses and di is the separate desirability value of each response resulted from the transformation of the individual response of each test. The individual desirability function orders were between di = 0 for a fully undesired response and di = 1 for a completely desired response. For a value of "*D*" near 1, response values are closed to the target parameters.

In this study, the main forces that dictated the responses are a minimization of particle size and maximization of enzyme activity. For these purposes, MCO was used, based on the desirability index of Derringer and carried out via the computer program (Design-Expert software 6.0.10). It appeared that the most significant factors that influenced the enzyme activity were the surfactant type, lipid type, and lipid/protein ratio, respectively. On the other hand, only the lipid/protein ratio had a significant effect on particle size. The best solution for the optimal conditions specified in $A = 50$, $B =$ behenic acid, and $C =$ Pluronic F-127 derived from the differentiation of quadratic models are given in Eqs. (1) and (2). The predicted optimal particle size and enzyme activity corresponding to these values were 395.9 nm and 95.95%, for this top solution, respectively. This condition within the range of experimental values (i.e., $D = 0.984$) corresponds to the maximum desirability function. To confirm the model adequacy, three additional experiments based on this optimum condition were carried out. The three replicate experiments yielded an average particle size and enzyme activity of 411 ± 12.6 nm and 92.1 ± 1.4%, respectively. Appropriate agreement between the predicted and experimental results verifies the validity of the models and the existence of the optimal points.

Determination of suitable surfactant concentration

After an experimental design investigation, to evaluate the proper concentration of pluronic F-127, three different concentrations of pluronic F-127 were used for preparing micellar nanocarrier. Based on the past studies on pluronic F-127 [39], the CMC value of this nonionic surfactant in the water at 25 °C is 0.55 mM. Results from Table 3 demonstrated that the 0.79-mM concentration of pluronic F-127 show the significant smaller particle size and also retained the enzyme activity better than the other two concentrations. Therefore, we used the 0.79-mM concentration of pluronic F-127 for subsequent investigations.

In vitro characterization tests

Stability to proteolysis and determination of pH-activity profile

The stability of native L-ASNase and micellar nanocarriers against trypsin digestion is shown in Fig. 2b. Micellar nanocarriers demonstrated higher stability against trypsin digestion than the native forms of the enzyme. The free form of the enzyme has low stability and, after 10 min of the reaction, lost half of its original activity; 86.2% of the initial activity of the native enzyme was reduced after 30 min, whereas the micellar nanocarrier retained about 70% of enzyme activity at the same time. The micellar nanocarriers kept more than half of their original activities during the 60 min of incubation in trypsin solution. It is known that the peptide bonds consisting of lysine or arginine residues are selectively hydrolyzed by trypsin [12]. Two different mechanisms may lead to the increase in proteolysis stability which include, (a) the steric hindrance effect of the fatty acids which protect the modified enzyme from the contact with protease, and so on the proteolysis reaction was prevented; (b) the modification of L-ASNase lysine residues with fatty acids may prevent selective proteolysis reaction on the peptide bonds with lysine residues. Furthermore, many hypotheses have proposed the possible effect of nonionic surfactant on maintaining the protein's native state. It is suggested that surfactants with their amphiphilic properties can compete with the enzyme for a denaturing

Table 3 Optimum pluronic F-127 concentration, calculated CMC, particle sizes, and polydispersity index (PDI) for the micellar nanocarriers after reconstitution of the lyophilizes

L-ASNase-fatty acid bioconjugate	Pluronic F-127 conc. (mM)	Enzyme activity %	Particle size (nm)	PDI	Calculated CMC by the DuNouy ring tensiometer (mM)
Pluronic F-127					0.582 ± 0.09
Behenic acid bioconjugate	0.79	92.06 ± 1.35	388 ± 9.85	0.34 ± 0.03	0.441 ± 0.082
	0.55	86.72 ± 2.76	831 ± 294.08	0.64 ± 0.16	
	0.079	75.57 ± 3.18	1344 ± 227.69	0.58 ± 0.36	
Palmitic acid bioconjugate	0.79	81.66 ± 2.50	344 ± 12.60	0.25 ± 0.19	0.462 ± 0.043
	0.55	74.28 ± 2.73	661 ± 44.01	0.69 ± 0.13	
	0.079	67.59 ± 2.06	1258 ± 117.38	0.72 ± 0.04	
Lauric acid bioconjugate	0.79	74.93 ± 1.44	422 ± 7.71	0.39 ± 0.10	0.441 ± 0.082
	0.55	71.12 ± 2.72	826 ± 318.05	0.80 ± 0.16	
	0.079	65.53 ± 2.10	4718 ± 17.68	0.66 ± 0.40	

surface and stop the surface-induced denaturation, specifically when added to a protein solution. Other investigations suggest that the surfactant can lower the Gibbs free energy of the system and increase the native enzyme conformation's stability by minimizing the potential energy of a surfactant-adsorbed protein through weak hydrophobic bonding [40]. Therefore, the micellar nanocarriers may present better stability than the native and even L-ASNase-fatty acid bioconjugate.

In this experiment, phosphate buffer with pH from 3.0 to 12.0 was used to investigate the influence of pH on the activities of native L-ASNase and micellar nanocarriers (Fig. 2a). The pH range was 6.5 to 9 for the modified enzyme, which was significantly broader than that for the native enzyme (7.5 to 8.5). The mechanism of protein stability in this wide range of the pH might be as a result of active site preservation [11, 41].

Kinetic measurements and time-activity profile in PBS and plasma

The Lineweaver-Burk plots for the native and micellar nanocarriers are shown in Table 4. For the native and micellar nanocarriers, four linear equations were obtained. As shown in Table 4, micellar nanocarriers showed smaller values of the K_m and higher affinity for the substrate compared to the native form. The difference in K_m constant between micellar nanocarriers and native form may be attributed to the limited accessibility of substrate to the active site of the modified enzyme due to the changes in protein conformation, steric hindrance, and diffusional effects [42, 43]. In the process of an enzymatic reaction, the substrate interacts with the enzyme to produce a substrate–enzyme intermediate. Following the formation of the intermediate complex, the release of the enzyme is performed and is recycled back to react with more

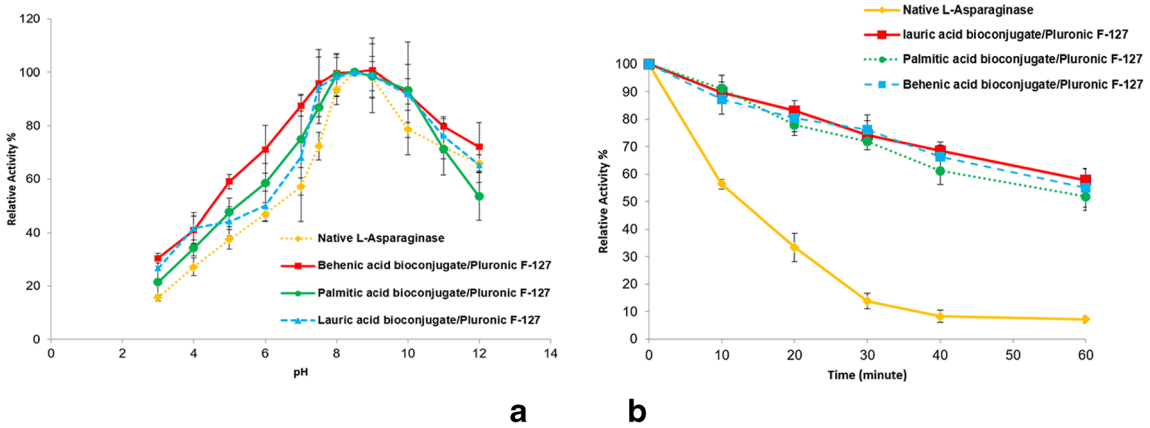

Fig. 2 **a** Effect of different pH on the activity of the optimized formulation in comparison with native LASNase. The highest activity has been set as 100% activity. **b** The relative activity of the optimized formulation in comparison with native L-ASNase after trypsin digestion (pH 8.5, 50 IU trypsin, 37 °C). The highest activity of native and modified L-asparginase has been set as 100%

Table 4 The in vitro half-lives, kinetic parameter, and zeta potential of the optimized formulation in comparison with native L-ASNase

Modified L-ASNase	Zeta potential (mV)	K_m (mM)	PBS		Plasma	
			$t_{½}$ (h)	K (h)	$t_{½}$ (h)	K (h)
Native L-ASNase	− 21.2	3.83 ± 1.79	22.12 ± 4.76	0.032 ± 0.008	19.14 ± 1.71	0.036 ± 0.003
L-ASNase-Lauric acid bioconjugate/PF-127	− 2.50	1.03 ± 0.53	20.41 ± 2.15	0.034 ± 0.004	48.26 ± 3.14	0.014 ± 0.001
L-ASNase-palmitic acid bioconjugate/PF-127	− 4.38	2.05 ± 0.99	40.55 ± 10.07	0.018 ± 0.004	49.81 ± 11.52	0.014 ± 0.004
L-ASNase-Behenic acid bioconjugate/PF-127	− 8.12	0.80 ± 0.08	44.90 ± 2.59	0.015 ± 0.001	60.00 ± 16.86	0.012 ± 0.004

substrate molecules. Thus, in this study, while conjugation and micellization decrease K_m, enzyme substrate-mediated production may be simplified (due to higher substrate affinity for the enzyme).

A longer in vitro half-life for L-ASNase is desirable because more clinical effectiveness can be achieve by maintaining higher human plasma concentration. The results of native L-ASNase and micellar nanocarrier stability towards PBS and human plasma are summarized in Table 4 that was achieved by the first-order model.

The native enzyme loaded in human plasma without ALL exhibited a reduction of 68.97 ± 6.27% in enzymatic activity after 10 h. This fact is explained by the presence of non-specific antibodies or proteases in human plasma being capable of inactivating L-ASNase. In order to verify if the enzyme modified with fatty acid and surfactant presented in this work results in more excellent enzyme stability in the same conditions, the micellar nanocarriers were mixed to the same human plasma samples. The modified enzyme retained its activity for 96 h when it was incubated in the same manner. These results suggest that the modification with fatty acid and pluronic F-127 protects L-ASNase by a steric hindrance to the binding of non-specific antibodies or at enzymatic hydrolysis caused by proteases in human plasma [9, 44]. Optimized formulation (L-ASNase- behenic acid bioconjugate/pluronic F-127), because of sterically stabilizing effect of pluronic F -127 [45], can circulate in the blood for extended time periods (2.1 times longer half-life) in comparison to the native enzyme.

Determination of CMC, particle size, size distribution, and surface charge

The comprehensive set of CMC results for pluronic F-127 and micellar nanocarriers are presented in Table 3. The surface tension is plotted vs. surfactant concentration for the determination of CMC. For each of the systems, a drop in surface tension was observed at a certain concentration. The tangent intersection points are drawn on the two curved sections denoted as CMC [46–48]. The CMC value of the micellar nanocarriers is significantly lower than the CMC of the pluronic F-127 alone. Since bioconjugate space out the individual surfactant molecules, it may reduce the repulsion and make it easier to incorporate monomeric surfactant molecules into micelles. This may effectively remove most of the active monomeric surfactant from the solution and allows us to focus on micellar effects [49].

The results of particle size and surface charge of the micellar nanocarriers are shown in Tables 3 and 4, respectively. In this study, the particles in terms of both central tendency indices and dispersity indices were uni-disperse (unimodal curves). In micellar nanocarriers, the pluronic F-127 has a superior effect on the size and charge reduction. This result is following other investigations on pluronic F-127 along with nanoparticles [45, 50].

Morphology

Similar to the results from the light scattering method, the morphological studies (Fig. 3) also demonstrated the uni-dispersed particle size and size distribution of the nanostructured carriers while showing a spherical shape for the optimized formulation (i.e., behenic acid bioconjugate/pluronic F-127). Notably, the smaller particle sizes and narrow size distribution for the behenic acid bioconjugate/pluronic F-127 was obtained in comparison with L-ASNase-behenic acid bioconjugate.

Pharmacokinetic analysis

A pharmacokinetic study was carried out by formulating administration to animals via a catheter inserted intravenously. In general, a comparative pharmacokinetic experiment was carried out by determining drug levels in serum up to 24 h after i.v. administration. The half-life of the behenic acid bioconjugated samples was about 1.5 times, and its related micellar nanocarrier (the optimized formulation) was two times longer than the half-life of the native L-ASNase ($n = 3$, $P < 0.05$). Also, the in vitro half-life of bioconjugated and micellar nanocarrier of L-ASNase demonstrated that fatty acid conjugation and combination with surfactant could increase the $t_{1/2}$ of L-ASNase (Fig. 4). It is also shown that the clearance of behenic acid bioconjugate and behenic acid

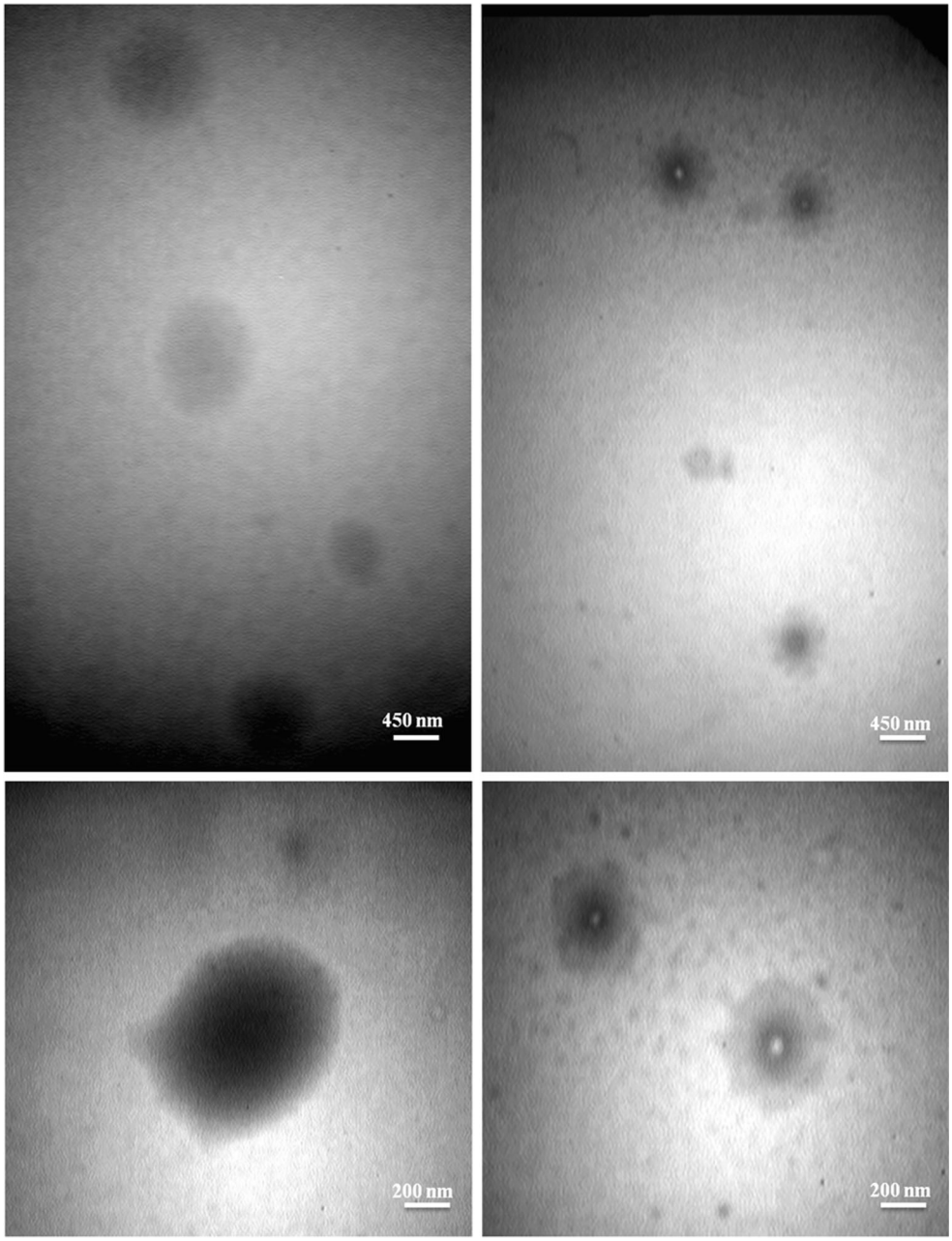

Fig. 3 TEM images of L-ASNase-fatty acid bioconjugate (0.1 mg/mL of enzyme) (left side) and L-ASNase-behenic acid bioconjugate/pluronic F-127 (0.1 mg/mL of enzyme) (right side)

bioconjugate/pluronic F-127 is changed significantly. Clearance of the behenic acid bioconjugate/pluronic F-127 was significantly lower than the clearance of the native and its relevant bioconjugated form. Moreover, a higher and significant increase in vivo half-life can be detected in L-ASNase-behenic acid bioconjugate, and its micellar nanocarrier compares to the native enzyme (Fig. 4). This observation can be explained by some suppressing effect on drug elimination as a result of conjugation and using a surfactant. As mentioned before, the in vitro results also showed the more stability of L-ASNase-fatty acid bioconjugate and related micellar nanocarriers to proteolysis and also presented longer activity half-lives. The long-term circulation of the drug observed in this study is probably due to the effect of surfactant. On account of surfactant treatment, the rate of the nanocarrier uptake by the natural body phagocyting cells and the reticuloendothelial system (RES) may reduce [51]. This phenomenon is a possible explanation for the long-lasting effect of the behenic acid bioconjugate/pluronic F-127. MRT values are about 1.4- and 2.2-fold higher than the native L-ASNase for behenic acid bioconjugate and its related micellar nanocarrier, respectively (Fig. 4). The lower RES uptake can explain it following the surface treatment with hydrophilic surfactants. These results were also confirmed by MRT values of the bioconjugated and micellar nanocarrier of the enzyme.

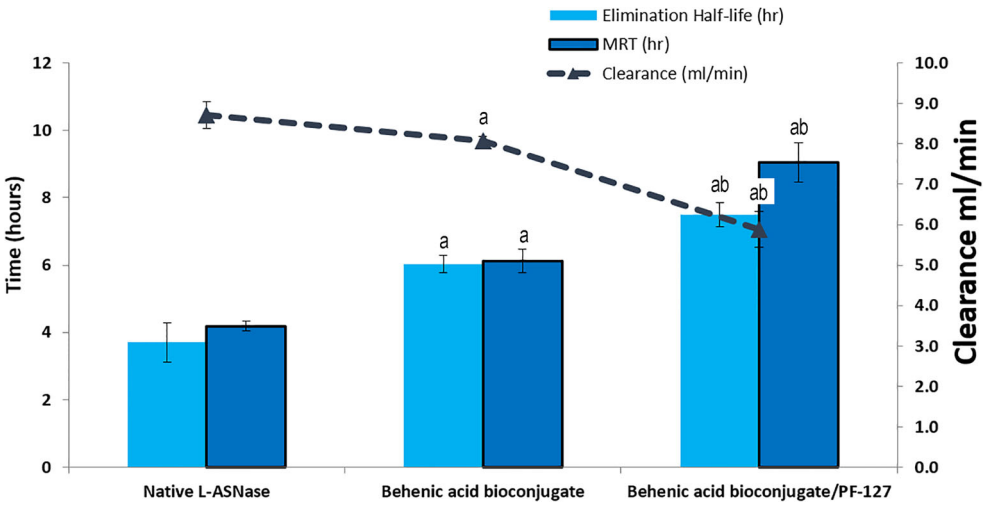

Fig. 4 Elimination half-life and mean residence time (MRTinf) and clearance of L-ASNase following i.v. administration of native enzyme, behenic acid bioconjugates, and optimum micellar nanocarrier (50:1 lipid:protein ratio) at the dose of 10 mg/kg; **a** significant with native L-ASNase; **b** significant with related fatty acid bioconjugate

Conclusion

Today, micellar nanocarrier, owing to their advantages, have dominated drug delivery efforts. They exhibit properties such as smaller particle size and higher stability superior to those of the mono-micellar system, emulsion, and nanoparticles. In this study, a simple and readily available preparation method was set up, optimized, and validated successfully via the systematic multi-criteria optimization approach in terms of the final particle size and enzyme activity for the fabrication of L-ASNase-fatty acid bioconjugate micellar nanocarrier. A series of in vitro characterization tests were carried out on the optimized micellar nanocarrier (behenic acid bioconjugate/pluronic F-127). The optimized formulation showed increased in vitro half-life, lengthened the range of optimum pH of activity, and advance proteolysis stability. Alteration of L-ASNase with fatty acid and surfactants also indicates a promising stabilized product for in vivo experiments. This study explains the new delivery candidate for the medical purposes of L-ASNase in the future.

Acknowledgments The authors would like to thank Mr. Omid Koohi-Hosseinabadi for his assistance in the animal experiments.

Funding This study was supported by Shiraz University of Medical Sciences (Grant No. 90-5980, Weiss, University of Research and Technology).

Compliance with ethical standards

Conflict of interest The authors declare that they have no conflict of interest.

References

1. Ashihara Y, Kono T, Yamazaki S, Inada Y (1978) Modification of *E. coli* L-asparaginase with polyethylene glycol: disappearance of binding ability to anti-asparaginase serum. Biochem Biophys Res Commun 83(2):385–391
2. Chen S-H (2015) Asparaginase therapy in pediatric acute lymphoblastic leukemia: a focus on the mode of drug resistance. Pediatr Neonatol 56(5):287–293
3. Vervliet T, Parys JB (2019) L-Asparaginase-induced apoptosis in ALL cells involves IP3 receptor signaling. Cell Calcium 83:102076
4. Graham ML (2003) Pegaspargase: a review of clinical studies. Adv Drug Deliv Rev 55(10):1293–1302
5. Muneer F, Siddique MH, Azeem F, Rasul I, Muzammil S, Zubair M, Afzal M, Nadeem H (2020) Microbial L-asparaginase: purification, characterization and applications. Arch Microbiol 202(1):967–981
6. Shrivastava A, Khan AA, Khurshid M, Kalam MA, Jain SK, Singhal PK (2016) Recent developments in l-asparaginase discovery and its potential as anticancer agent. Crit Rev Oncol Hematol 100(1):1–10
7. Cristóvão RO, Almeida MR, Barros MA, Nunes JCF, Boaventura RAR, Loureiro JM, Faria JL, Neves MC, Freire MG, Ebinuma-Santos VC (2020) Development and characterization of a novel L-asparaginase/MWCNT nanobioconjugate. RSC Adv 10(52):31205–31213
8. Fernandes AI, Gregoriadis G (2001) The effect of polysialylation on the immunogenicity and antigenicity of asparaginase: implication in its pharmacokinetics. Int J Pharm 217(1–2):215–224
9. Zhang Y-Q, Zhou W-L, Shen W-D, Chen Y-H, Zha X-M, Shirai K, Kiguchi K (2005) Synthesis, characterization and immunogenicity of silk fibroin-l-asparaginase bioconjugates. J Biotechnol 120(3):315–326
10. Zhang YQ, Tao ML, Shen WD, Mao JP, Chen Y (2006) Synthesis of silk sericin peptides–L-asparaginase bioconjugates and their characterization. J Chem Technol Biotechnol 81(2):136–145
11. Tabandeh MR, Aminlari M (2009) Synthesis, physicochemical and immunological properties of oxidized inulin-L-asparaginase bioconjugate. J Biotechnol 141(3–4):189–195
12. Guoqiang Q, Juyan Z, Jianbiao M, Binglin H, Daobin W (1997) Chemical modification of L-asparaginase with N,O-carboxymethyl chitosan and its effects on plasma half-life and other properties. Science in China 40(4):337–341
13. Chahardahcherik M, Ashrafi M, Ghasemi Y, Aminlari M (2020) Effect of chemical modification with carboxymethyl dextran on kinetic and structural properties of L-asparaginase. Anal Biochem 591:113537
14. Baskar G, Lalitha K, Garrick BG, Chamundeeswari M (2017) Conjugation, labeling and characterization of asparaginase bound silver nanoparticles for anticancer applications

15. Agrawal S, Sharma I, Prajapati BP, Suryawanshi RK, Kango N (2018) Catalytic characteristics and application of l-asparaginase immobilized on aluminum oxide pellets. Int J Biol Macromol 114:504–511
16. Do TT, Do TP, Nguyen TN, Nguyen TC, Vu TTP, Nguyen TGA (2019) Nanoliposomal L-asparaginase and its antitumor activities in Lewis lung carcinoma tumor-induced BALB/c mice. Adv Mater Sci Eng 2019(1):2–9
17. Orhan H, Uygun DA (2020) Immobilization of L-asparaginase on magnetic nanoparticles for cancer treatment. Appl Biochem Biotechnol 191:1432–1443
18. Ashrafi H, Amini M, Mohammadi-Samani S, Ghasemi Y, Azadi A, Tabandeh MR, Kamali-Sarvestani E, Daneshamouz S (2013) Nanostructure l-asparaginase-fatty acid bioconjugate: synthesis, preformulation study and biological assessment. Int J Biol Macromol 62:180–187
19. Hamidi M, Ashrafi H, Azadi A (2012) Surface functionalized hydrogel nanoparticles. In: Tiwari A, Ramalingam M, Kobayashi H, Turner APF (eds) Biomedical materials and diagnostic devices. John Wiley & Sons, Beverly
20. Singh Bakshi M, Singh J, Kaur G (2005) Mixed micelles of monomeric and dimeric cationic surfactants with phospholipids: effect of hydrophobic interactions. Chem Phys Lipids 138:81–92
21. Kakehashi R, Shizuma M, Yamamura S, Takeda T (2004) Mixed micelles containing sodium oleate: the effect of the chain length and the polar head group. J Colloid Interface Sci 279(1):253–258
22. Leiro J, Siso MIG, Ortega M, Santamarina MT, Sanmartin ML (1995) A factorial experimental design for investigation of the effects of temperature, incubation time, and pathogen-to-phagocyte ratio on *in vivo* phagocytosis by turbot adherent cells. Comp Biochem Physiol C Toxicol Pharmacol 112(2):215–220
23. Barati M, Samani SM, Jahromi LP, Ashrafi H, Azadi A (2018) Controlled-release in-situ gel forming formulation of tramadol containing chitosan-based pro-nanogels. Int J Biol Macromol 118: 1449–1454
24. Sharma G, Goyal AK, Singh AP (2019) Application of design of expert for the development and systematic optimisation of L-asparaginase loaded nanoparticulate carrier drug delivery systems. J Drug Deliv Ther 9(3-s):303–308
25. Hermanson GT (ed) (2008) Bioconjugate techniques, 2nd edn. Academic Press, Oxford
26. Itaya K (1977) A more sensitive and stable colorimetric determination of free fatty acids in blood. J Lipid Res 18(5):663–665
27. Ashrafi H, Azadi A, Mohammadi-Samani S, Ghasemi Y, Daneshamouz S (2020) Preliminary study for the preparation of fatty acid bioconjugated L-asparaginase micellar nanocarrier as a delivery system for peptide anti-cancer agents. Trends Pharmacol Sci 6(3):175–188
28. Azadi S, Ashrafi H, Azadi A (2017) Mathematical modeling of drug release from swellable polymeric nanoparticles. J Appl Pharm Sci 7(04):125–133
29. Habeeb AFSA (1966) Determination of free amino groups in proteins by trinitrobenzenesulfonic acid. Anal Biochem 14(3):328–336
30. Abdellatef HE, Khalil HM (2003) Colorimetric determination of gabapentin in pharmaceutical formulation. J Pharm Biomed Anal 31(1):209–214
31. Wang R, Xia B, Li BJ, Peng SL, Ding LS, Zhang S (2008) Semipermeable nanocapsules of konjac glucomannan-chitosan for enzyme immobilization. Int J Pharm 364(1):102–107
32. Ghosh S, Chaganti SR, Prakasham RS (2012) Polyaniline nanofiber as a novel immobilization matrix for the anti-leukemia enzyme l-asparaginase. J Mol Catal B Enzym 74(1–2):132–137
33. Bradford MM (1976) A rapid and sensitive method for the quantitation of microgram quantities of protein utilizing the principle of protein-dye binding. Anal Biochem 72:248–254
34. Jambhekar SS, Breen PJ (2009) Basic pharmacokinetics. Pharmaceutical Press, London
35. Waynforth H, Flecknell P (1992) Experimental and surgical techniques in the rat
36. Miron J, Siso MIG, Murado MA, Gonzalez MP (1988) Microfungus-yeast mixed cultures in the degradation of amylaceous wastes. II An experimental design for optimization of yeast production. Biotechnol Lett 2(1):171–176
37. Deming SN (1991) Multiple-criteria optimization. J Chromatogr A 550(1):15–25
38. Derringer G, Suich R (1980) Simultaneous optimization of several response variables. J Qual Technol 12(4):214–219
39. Gao Q, Liang Q, Yu F, Xu J, Zhao Q, Sun B (2011) Synthesis and characterization of novel amphiphilic copolymer stearic acid-coupled F127 nanoparticles for nano-technology based drug delivery system. Colloids Surf B Biointerfaces 88(2):741–748
40. England JL (1999) Stabilization and release effects of Pluronic F127 in protein drug delivery. Juventudes Univ Socialistas 5(1): 17–24
41. Soares AL, Guimarães GM, Polakiewicz B, Pitombo RNM, Abrahão-Neto J (2002) Effects of polyethylene glycol attachment on physicochemical and biological stability of *E. coli*-asparaginase. Int J Pharm 237(1–2):163–170
42. Eldin M, Portaccio M, Diano N, Rossi S, Bencivenga U, D'Uva A, Canciglia P, Gaeta FS, Mita DG (1999) Influence of the microenvironment on the activity of enzymes immobilized on Teflon membranes grafted by γ-radiation. J Mol Catal B Enzym 7(5):251–261
43. Arica MY, Hasirci V (1993) Immobilization of glucose oxidase: a comparison of entrapment and covalent bonding. J Chem Technol Biotechnol 58(3):287–292
44. Jorge JCS, Perez-Soler R, Morais JG, Cruz MEM (1994) Liposomal palmitoyl-L-asparaginase: characterization and biological activity. Cancer Chemother Pharmacol 34(3):230–234
45. Dumortier G, Grossiord JL, Agnely F, Chaumeil JC (2006) A review of poloxamer 407 pharmaceutical and pharmacological characteristics. Pharm Res 23(12):2709–2728
46. Murphy A, Taggart G (2002) A comparison of predicted and experimental critical micelle concentration values of cationic and anionic ternary surfactant mixtures using molecular-thermodynamic theory and pseudophase separation theory. Colloids Surf A Physicochem Eng Asp 205(3):237–248
47. Akhter MS, Alawi SM (2000) The effect of organic additives on critical micelle concentration of non-aqueous micellar solutions. Colloids Surf A Physicochem Eng Asp 175(3):311–320
48. Burlatsky SF, Atrazhev VV, Dmitriev DV, Sultanov VI, Timokhina EN, Ugolkova EA, Tulyani S, Vincitore A (2013) Surface tension model for surfactant solutions at the critical micelle concentration. J Colloid Interface Sci 393(1):151–160
49. Otzen D (2011) Protein–surfactant interactions: a tale of many states. Biochim Biophys Acta 1814(5):562–591
50. Vidya J, Ushasree MV, Pandey A (2014) Effect of surface charge alteration on stability of L-asparaginase II from Escherichia sp. Enzym Microb Technol 56:15–19
51. Zhao Z, Ukidve A, Krishnan V, Mitragotri S (2019) Effect of physicochemical and surface properties on *in vivo* fate of drug nanocarriers. Adv Drug Deliv Rev 143(1):3–21